

Charge and spin Drude weight of the one-dimensional extended Hubbard model at quarter filling

Tomonori Shirakawa

*Graduate School of Science and Technology, Chiba University, Chiba 263-8522, Japan
and Institut für Theoretische Physik, Leibniz Universität Hannover, Appelstrasse 2, D-10607 Hannover, Germany*

Eric Jeckelmann

*Institut für Theoretische Physik, Leibniz Universität Hannover, Appelstrasse 2, D-10607 Hannover, Germany
(Received 24 February 2009; revised manuscript received 20 April 2009; published 22 May 2009)*

We calculate the charge and spin Drude weight of the one-dimensional extended Hubbard model with on-site repulsion U and nearest-neighbor repulsion V at quarter filling using the density-matrix renormalization-group method combined with a variational principle. Our numerical results for the Hubbard model ($V=0$) agree with exact results obtained from the Bethe ansatz solution. We obtain the contour map for both Drude weights in the UV -parameter space for repulsive interactions. We find that the charge Drude weight is discontinuous across the Kosterlitz-Thouless transition between the Luttinger liquid and the charge-density-wave insulator, while the spin Drude weight varies smoothly and remains finite in both phases. Our results can be generally understood using bosonization and renormalization-group results. The finite-size scaling of the charge Drude weight is well fitted by a polynomial function of the inverse system size in the metallic region. In the insulating region, we find an exponential decay of the finite-size corrections with the system size and a universal relation between the charge gap Δ_c and the correlation length ξ which controls this exponential decay.

DOI: [10.1103/PhysRevB.79.195121](https://doi.org/10.1103/PhysRevB.79.195121)

PACS number(s): 71.10.Fd, 71.10.Hf, 71.10.Pm

I. INTRODUCTION

The transport properties of low-dimensional strongly correlated electron systems are currently a subject of great interest because of recent experimental observations in quasi-one-dimensional (quasi-1D) materials and because of their connection to the rapidly evolving field of nonequilibrium physics in strongly correlated quantum systems.¹ Most studies of transport properties in one-dimensional quantum many-body systems have been within the linear-response theory.² One fundamental quantity is the Drude weight defined as the zero-frequency contribution to the real part of the conductivity. Thus a finite Drude weight implies ballistic transport, and it has been proposed as a criterion for distinguishing metallic and insulating phases in a Mott transition.³

Experiments on quasi-one-dimensional organic conductors⁴ show large deviations from the predictions of band theory. According to previous studies, the intersite Coulomb repulsion plays a crucial role in these materials.⁵ Therefore, the most simple effective model for their electronic properties is a one-dimensional extended Hubbard model. In such one-dimensional models of interacting fermions, the quasiparticle concept breaks down, and the properties of the system do not resemble those of a Fermi liquid. Instead, low-energy excitations are made of independent elementary excitations for spins (spinons) and charge (holons).^{6,7} Moreover, the space- and time-dependent correlation functions display unusual power-law decays. Their exponents are not universal but depend on the strength of the interaction. One-dimensional metallic systems belong to the generic class of Tomonaga-Luttinger liquids (TLL).⁸⁻¹¹ Their characteristic quantities are the so-called TLL parameters v_ρ , v_σ , K_ρ , and K_σ . Here v_ρ and v_σ are the velocity of charge and spin excitations, respectively, and K_ρ and K_σ determine the algebraic decay of correlation functions.

Recently, the discovery of the colossal magnetic heat transport in spin ladder materials, such as $(\text{Sr,Ca,La})_{14}\text{Cu}_{24}\text{O}_{41}$, where the magnetic contribution to the total thermal conductivity exceeds the phonon contribution substantially, has sparked interest in transport properties of quasi-1D spin models.¹²⁻¹⁴ Understanding the transport properties of theoretical models is of great importance for the interpretation of transport or NMR measurements, but it is still an open problem for quantum systems involving many coupled degrees of freedom.^{1,15} Therefore, the development of methods for computing transport properties such as the Drude weight in strongly correlated systems and the investigation of these properties are much anticipated.

In this paper we study the charge and spin Drude weight of the one-dimensional extended Hubbard model at quarter filling using the density-matrix renormalization-group (DMRG) method with periodic boundary conditions. This model is known to be “nonintegrable” for general values of the parameters¹⁶ and thus not amenable to an exact calculation of the Drude weight contrary to the Hubbard model.¹⁷ Investigations based on the g -ology,⁸ bosonization,¹⁸⁻²⁰ and the renormalization group^{21,22} have provided analytic insight, particularly, in the weak-coupling regime. Both exact diagonalization²³⁻²⁷ calculations and quantum Monte Carlo simulations²⁸ have clarified a number of questions at intermediate and strong coupling. In the last decade, the DMRG method has been successfully used to investigate many properties of one-dimensional strongly correlated lattice models,^{29,30} but a precise calculation of charge and spin Drude weights has not been reported yet. Therefore, we still lack a comprehensive picture of ballistic transport in the one-dimensional extended Hubbard model.

Our paper is organized as follows. In Sec. II, we summarize some properties of the extended Hubbard model and its

ground-state phase diagram and introduce the charge and spin Drude weight. In Sec. III, we explain the DMRG-based method for calculating the Drude weight. Our results for the thermodynamic limit are presented in Sec. IV A and the finite-size scaling is discussed in detail in Sec. IV B. Finally, we summarize our work in the last section.

II. MODEL AND DRUDE WEIGHT

We study the one-dimensional extended Hubbard model which is defined by the Hamiltonian

$$H = H_t + H_U, \quad (1)$$

$$H_t = -t \sum_{l,\sigma} (c_{l,\sigma}^\dagger c_{l+1,\sigma} + c_{l+1,\sigma}^\dagger c_{l,\sigma}), \quad (2)$$

$$H_U = U \sum_l n_{l,\uparrow} n_{l,\downarrow} + V \sum_l n_l n_{l+1}, \quad (3)$$

where $c_{l,\sigma}^\dagger$ ($c_{l,\sigma}$) is the creation (annihilation) operator for an electron with spin σ ($=\uparrow, \downarrow$) at site $l=1, \dots, L$, $n_{l,\sigma} = c_{l,\sigma}^\dagger c_{l,\sigma}$ is the density operator, and $n_l = n_{l,\uparrow} + n_{l,\downarrow}$. We use periodic boundary conditions throughout. $t > 0$ is the nearest-neighbor hopping integral along the chain, $U \geq 0$ is the onsite Coulomb interaction, and $V \geq 0$ is the nearest-neighbor Coulomb interaction. A quarter-filled band corresponds to a system with $N=L/4$ electrons of each spin, a Fermi wave vector $k_F = \frac{\pi}{4}$, and a Fermi velocity $v_F = 2t \sin(k_F) = \sqrt{2}t$ in the Fermi gas ($U=V=0$).

This model has been studied extensively by a variety of techniques. It is known to be “nonintegrable” for general values of the parameters¹⁶ on the basis of energy-level statistics, although exact results can be obtained in three limits ($V=0$, $U=+\infty$, $V=+\infty$). For $V=0$, the model becomes the regular Hubbard model. At quarter filling, it is known to be metallic³¹ with dominant $2k_F$ -spin-density-wave (SDW) fluctuations, and its low-energy excitations are of the TLL type. For $U=+\infty$, the quarter-filled electron model is equivalent to a half-filled spinless fermion model which upon increasing V from zero undergoes a phase transition from a TLL phase to a $4k_F$ -charge-density-wave (CDW) insulator at $V=2t$.³² For $V=+\infty$, onsite electron pairs cannot move, while the unpaired electrons have the same kinetic energy as spinless fermions interacting with an infinitely strong nearest-neighbor repulsion. This system has a Bethe ansatz solution.^{24,25,33,34} It is a $4k_F$ -CDW insulator for $U > U_c = 4t$, whereas it is phase separated for $U < U_c$. In the weak-coupling limit ($U, V \ll t$), the model can be mapped onto a g -ology model and investigated using bosonization and renormalization-group techniques.^{8,18–22}

The ground-state phase diagram of the quarter-filled extended Hubbard model for repulsive interactions was first determined using exact diagonalizations.²⁴ Recently, the precise ground-state phase diagram and the TLL exponent K_ρ have been obtained for a wide region of the UV -parameter space using the DMRG method.³⁰ These results are summarized in Fig. 1, where four different phases are represented: (I) a metallic phase with $1/3 \leq K_\rho \leq 1$ where the system has

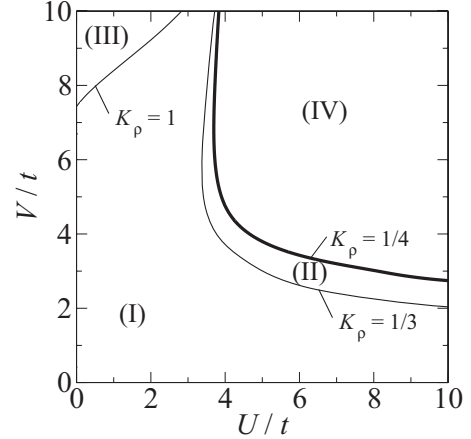


FIG. 1. The phase diagram of the t - U - V model at quarter filling determined from DMRG calculations in Ref. 30. In region (i), $1/3 < K_\rho < 1$ and $2k_F$ -SDW correlations are dominant. Region (II) is characterized by dominant $4k_F$ -CDW correlation and $1/4 < K_\rho < 1/3$. In region (III), triplet pairing correlations dominate because of $K_\rho > 1$. The regions (i), (II), and (III) are metallic states, while region (IV) is an insulating state with $4k_F$ charge ordering.

dominant $2k_F$ -SDW fluctuations, (II) a metallic phase with $1/4 \leq K_\rho \leq 1/3$ where the system has dominant $2k_F$ -CDW fluctuations, (III) a metallic phase ($K_\rho \geq 1$) where the system has dominant superconducting fluctuations, and (IV) an insulating phase (i.e., with a finite charge gap) where the system has a long-range-ordered $4k_F$ CDW. All four phases have gapless spin excitations.^{24–26} Finite spin gaps have been reported in previous exact diagonalization studies for large V in phase (III), but our DMRG calculations indicate that the spin gap vanishes in the thermodynamic limit at least for all $V \leq 10t$. On the metal-CDW transition line $K_\rho = 1/4$. It has been reported that this transition is of the Kosterlitz-Thouless type,²⁶ and higher-order scattering processes, including the $8k_F$ -umklapp scattering via the upper band around $\pm 3k_F$, play a crucial role in the weak-coupling theory of the phase diagram.^{7,19,20,35}

Let us consider external fields ϕ_ρ and ϕ_σ which modify the kinetic energy

$$H_t(\phi_\rho, \phi_\sigma) = -t \sum_{l,\sigma} (e^{i(\phi_\rho + \sigma\phi_\sigma)L} c_{l+1,\sigma}^\dagger c_{l,\sigma} + \text{H.c.}). \quad (4)$$

ϕ_ρ is the magnetic flux threading the system and ϕ_σ is the magnetic flux given by a fictitious spin-dependent vector potential.³⁶ Time-dependent fields ϕ_μ generate a charge ($\mu = \rho$) or spin ($\mu = \sigma$) current $\langle J_\mu \rangle$ in the system. Within the linear-response theory, the charge and spin conductivities have the form^{15,37–40}

$$\text{Re } \sigma_\mu(\omega) = \pi D_\mu \delta(\omega) + \sigma_\mu^{\text{reg}}(\omega), \quad (5)$$

where $\sigma_\mu^{\text{reg}}(\omega)$ is assumed to be regular at $\omega=0$. The coefficient D_μ (D_σ) of the δ function $\delta(\omega)$ is called charge (spin) Drude weight for the ballistic transport and is given by

$$D_\mu = S_K + S_\mu = -\frac{1}{2L} \langle \psi_0 | H | \psi_0 \rangle - \frac{1}{L} \sum_n \frac{|\langle \psi_n | J_\mu | \psi_0 \rangle|^2}{E_n - E_0}, \quad (6)$$

where ψ_n denotes an eigenstate of H with energy E_n and the ground state corresponds to $n=0$. The first term (up to the prefactor $-1/2L$) is the total kinetic energy, while the second term (up to a prefactor $-\pi/2$) is the total spectral weight of the incoherent part $\sigma_\mu^{\text{reg}}(\omega)$ of the conductivity and describes the reduction in the Drude weight caused by incoherent-scattering processes. The charge and spin current operators are $J_\mu = \sum_i j_{\mu,i}$ with local current operators defined from the continuity equation

$$i[H, d_{\mu,l}] + j_{\mu,l+1} - j_{\mu,l} = 0, \quad (7)$$

where $d_{\rho,l} = n_l$ and $d_{\sigma,l} = n_{l,\uparrow} - n_{l,\downarrow}$. In our model, the precise form of $j_{\mu,l}$ is

$$j_{\rho,l} = -it \sum_\sigma c_{l+1,\sigma}^\dagger c_{l,\sigma} + \text{H.c.}, \quad (8)$$

$$j_{\sigma,l} = -it \sum_\sigma \sigma (c_{l+1,\sigma}^\dagger c_{l,\sigma} + \text{H.c.}). \quad (9)$$

The above spin current operator is different from the one used in spin models.^{15,41} Nevertheless, the spin Drude weights defined for an electron system or for a spin system have the same physical meaning because they characterize the response of the spin degrees of freedom to the same external perturbation. The spin Drude weight D_σ is thus defined as a precise analog of the charge Drude weight D_ρ . Therefore, a value $D_\sigma > 0$ simply means that the system is an ideal spin conductor, so that the spin transport is not diffusive.³⁷

Obviously, charge and spin Drude weight are equivalent in the noninteracting electron gas ($U=V=0$) because the second term of Eq. (6) vanishes. Assuming that the low-energy excitation of our model can be expressed by the TLL theory, the charge and spin Drude weight can be represented by¹¹

$$D_\mu = v_\mu K_\mu / \pi, \quad (10)$$

where v_ρ (v_σ) is the renormalized charge (spin) velocity and K_ρ (K_σ) is the renormalized TLL exponent of charge (spin) mode. In our model, the renormalized value of K_σ is $K_\sigma = 1$ because the system has a SU(2) spin symmetry and there is no spin gap in the repulsive parameter region. Thus, $\pi D_\sigma = v_\sigma$. On the other hand, the behavior of D_ρ is more complicated because v_ρ and K_ρ depend on the interaction parameters.

III. DMRG METHODS FOR DRUDE WEIGHTS

A method for calculating the Drude weight (6) with DMRG was introduced several years ago²⁹ but has been rarely used until now. In this section, we briefly summarize our implementation of this numerical method and discuss some technical details.

The first term of Eq. (6) can be easily calculated using the ground-state DMRG method. The second term can be calculated by targeting the correction vector $|\psi\rangle$ which is solution of

$$(H - E_0)|\psi\rangle = J_\mu|\psi_0\rangle. \quad (11)$$

The best implementation of this idea is a variational principle similar to the one used for the calculation of dynamical correlation functions.^{42,43} One considers the functional

$$W_\mu(\psi) = \langle \psi | (H - E_0) | \psi \rangle - \langle J_\mu | \psi \rangle - \langle \psi | J_\mu \rangle. \quad (12)$$

If the ground state is not degenerate, this functional has a unique minimum for the quantum state which is the solution of Eq. (11). It is easy to show that the value of the minimum is related to the second term of Eq. (6),

$$W_\mu(\psi_{\text{min}}) = - \sum_n \frac{|\langle \psi_n | J_\mu | \psi_0 \rangle|^2}{E_n - E_0}. \quad (13)$$

Our method consists in calculating the ground state and then minimizing this functional with DMRG. Note that this approach does not work for systems with a degenerated ground state. Therefore, we always choose appropriate system sizes L and numbers of electrons N to get a nondegenerate ground state.

Another approach for obtaining the Drude weight with DMRG is to compute the dynamical current-current correlation function

$$C_{\mu,\eta}(\omega) = - \langle \psi_0 | J_\mu \frac{1}{\omega + E_0 - H + i\eta} J_\mu | \psi_0 \rangle, \quad (14)$$

using the dynamical DMRG (DDMRG) method.^{42,43} The imaginary part of this quantity satisfies

$$\frac{1}{\omega} \lim_{\eta \rightarrow 0} \text{Im} C_{\mu,\eta}(\omega) = \sigma_\mu^{\text{reg}}(\omega), \quad (15)$$

which has been previously used to study the optical absorption of various one-dimensional insulators including the extended Hubbard model at half filling.⁴⁴ The real part of the correlation function yields

$$\lim_{\eta \rightarrow 0} \text{Re} C_{\mu,\eta}(0) = \sum_n \frac{|\langle \psi_n | J_\mu | \psi_0 \rangle|^2}{E_n - E_0}, \quad (16)$$

which can be expected from the Kramers-Kronig relation with the f -sum rule of conductivity. Therefore, one can in principle calculate the second term of Eq. (6) using DDMRG. However, a DMRG calculation using Eqs. (12) and (13) is faster and more accurate than a DDMRG calculation of Eqs. (14) and (15). In the first approach, the error in the value of the minimum $W_\mu(\psi_{\text{min}})$ is on the order of ϵ^2 if we can calculate target states with an error of the order $\epsilon \ll 1$ within DMRG. With the DDMRG method, the error in the real part of $C_{\mu,\eta}(\omega)$ is on the order of ϵ (see the discussion in Refs. 42 and 43).

As originally noted by Kohn,³ the Drude weight (6) can be calculated from the dependence of the ground-state energy on the applied field ϕ_μ using

$$D_\mu = L \left. \frac{\partial^2 E_0(\phi_\mu)}{\partial \phi_\mu^2} \right|_{\phi_\mu=0}. \quad (17)$$

Therefore, one can calculate the Drude weight with DMRG using Eq. (17). This approach has been demonstrated on the

spinless fermion model,^{29,45} but it requires treating complex Hamiltonians and performing a numerically delicate second derivative of the ground-state energy with respect to ϕ_μ . Therefore, we have chosen the approach based on the variational principle (12) and on Eq. (13).

IV. RESULTS

We have carried out DMRG calculations for quarter-filled chains with periodic boundary conditions and lengths up to $L=60$. The investigated system lengths are given by $L=8l+4$ with integers $l>1$ so that the number of electrons of each spin ($N=L/4$) is odd. Thus the ground state has momentum $P=0$ and is not degenerate. We have kept up to $m\approx 3200$ density-matrix eigenstates in the DMRG procedure. The discarded weights are typically on the order $10^{-6}\sim 10^{-8}$ and the ground-state energy accuracy is $\sim 10^{-4}t$. All energies and physical quantities are extrapolated to the limit $m\rightarrow\infty$.

A. Thermodynamic limit

We first discuss the DMRG results extrapolated to the thermodynamic limit ($L\rightarrow\infty$). The finite-size scaling is discussed in the next subsection. Contour maps of the charge and spin Drude weights are shown in Fig. 2. We can summarize our main results in five points. (i) Both D_ρ and D_σ have their maximum $D_\mu=v_F/\pi=\sqrt{2}t/\pi$ at the noninteracting point ($U=V=0$) and decrease monotonically as a function of increasing U and V . (ii) Excepted for the noninteracting point, we observe a difference between D_ρ and D_σ . (This is due to the well-known spin-charge separation, which is a typical property in one-dimensional systems.) (iii) The charge Drude weight has no linear correction around the noninteracting point $\partial D_\rho/\partial U=\partial D_\rho/\partial V=0$ at $U=V=0$. (iv) The charge Drude weight is larger than the spin Drude weight in the metallic phase. (v) D_ρ seems to be discontinuous at the metal-insulator transition. To understand these features, we will discuss the behavior of both Drude weights along the lines $V=0$, $U=0$, and $U=10t$ in more detail below.

Our DMRG calculation results for $V=0$ can be compared with the exact Drude weights D_μ^{exact} obtained from the Bethe ansatz solution of the Hubbard model¹⁷ as shown in Fig. 3. Relative errors $(D_\mu^{\text{exact}}-D_\mu^{\text{DMRG}})/D_\mu^{\text{exact}}$ are below 10^{-4} for each system size $L\leq 60$ using up to 3000 density-matrix states. We note that the charge Drude weight is larger than the spin Drude weight for all $U>0$ in Fig. 3. The reduction in both Drude weights for finite interactions can be understood qualitatively. The kinetic-energy term S_K in Eq. (6) is maximal for noninteracting electrons ($U=V=0$) and decreases monotonically when U (or V) increases. The second term S_μ in Eq. (6) equals 0 at the noninteracting point and can only decrease to negative values for $U>0$ (or $V>0$). (Note that S_μ is not a monotonic function of U and V . It has a minimum at finite interactions as it converges to zero in the strong-coupling limit.) Therefore, the decrease in the Drude weight is due to both the suppression of the kinetic energy and the appearance of scattering processes.

In Fig. 3 we can see in both our DMRG results and the exact Bethe ansatz results that D_ρ has no linear correction in

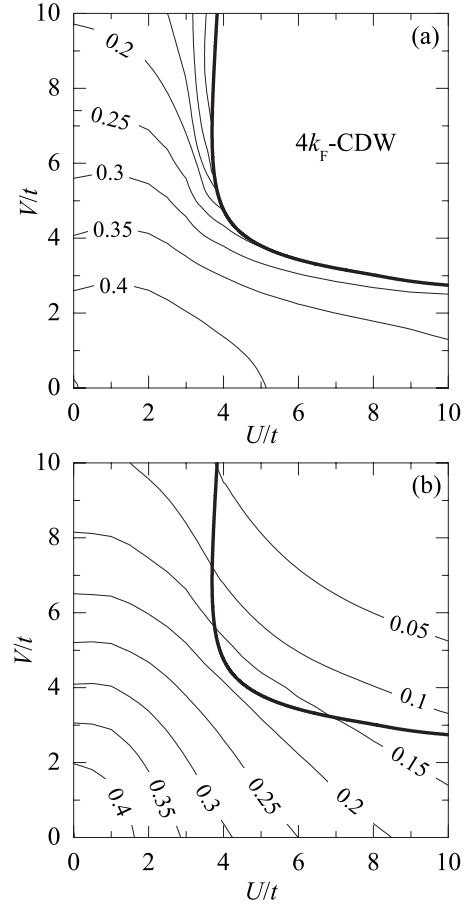


FIG. 2. Contour map for (a) the charge Drude weight D_ρ and (b) the spin Drude weight D_σ in the UV -parameter space of the extended Hubbard model at quarter filling. The bold line represents the boundary of the metal-insulator transition determined from K_ρ in Ref. 30.

U close to the noninteracting point ($U=0$), whereas D_σ seems to have a linear correction in U . This weak-coupling behavior has already been discussed.^{7,46,47} The renormalized value of K_σ is always $K_\sigma=1$ because there is no spin gap for the parameters investigated here. Therefore, the lowest-order correction to D_σ yields $D_\sigma=v_F/\pi-U/(2\pi^2v_F)$, which is also consistent with the Bethe ansatz result.⁴⁸ The behavior of K_ρ is more complicated.^{7,30} There is no first-order correction from the interaction U and thus if we neglect the irrelevant

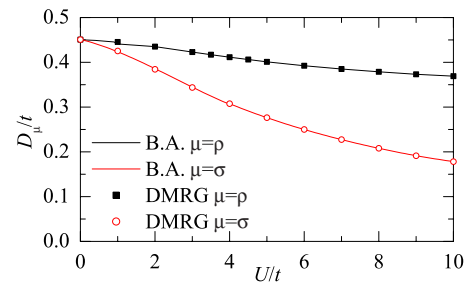


FIG. 3. (Color online) Charge Drude weight D_ρ and spin Drude weight D_σ as a function of U in the Hubbard model ($V=0$). Lines show the exact results from the Bethe ansatz solution.

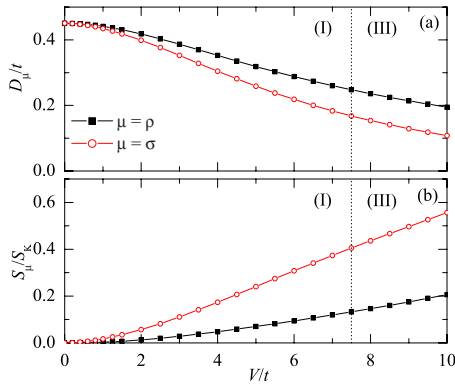


FIG. 4. (Color online) (a) The charge Drude weight D_ρ and spin Drude weight D_σ as a function of V along the $U=0$ line. (b) The ratio S_μ/S_K where S_K and S_μ are the first term and second term in Eq. (6), respectively. Vertical lines show the boundary between the Luttinger liquid phases with dominant SDW (i) and pairing (III) fluctuations. Other lines are guides for the eyes.

incommensurate $4k_F$ -umklapp scattering⁴⁶ and higher-order corrections in U ,¹⁹ $D_\rho = v_\rho K_\rho / \pi = v_F / \pi$. To understand the decrease of D_ρ , the effect of the irrelevant $4k_F$ -umklapp scattering has to be taken into account. This correction is second or higher order in the interaction and explains the nonlinear decrease of D_ρ . Note that if we neglect the irrelevant $4k_F$ -umklapp scattering but take higher-order corrections in U into account (see Ref. 19), D_ρ increases, which contradicts both our numerical results and the Bethe ansatz results. Thus, though those higher-order corrections are important for qualitatively understanding the phase diagram of this model, they are not sufficient for a quantitative analysis.

In the strong-coupling limit $U \rightarrow \infty$, we expect the following behavior: D_ρ approaches the value t/π because $v_\rho \rightarrow 2t \sin 2k_F = 2t$ and $K_\rho \rightarrow 1/2$, while D_σ goes to 0 because $v_\sigma \sim O(1/U)$. Therefore, along the $V=0$ line, D_ρ is larger than D_σ in both the $U \rightarrow 0$ and $U \rightarrow \infty$ limits and our DMRG results show that this relation holds also for all finite $U \geq 0$.

Results for the $U=0$ line of the UV -parameter space are shown in Fig. 4(a). Again we clearly see that both Drude weights decrease monotonically with increasing interaction and that the spin Drude weight is less than the charge Drude weight for all $V > 0$. In that case, however, it seems that both Drude weights have no linear correction in V at the noninteracting point ($U=V=0$). This is consistent with the weak-coupling theory which yields no correction to $v_\rho K_\rho$ or v_σ in the first order in V .¹¹ The faster reduction of D_σ with increasing V is due to the much stronger incoherent-scattering processes for spin excitations than for charge excitations, which is demonstrated by the larger second term S_μ of Eq. (6) as shown in Fig. 4(b).

We also find that S_μ/S_K increases in the Luttinger liquid phase (III) with dominant superconducting correlations, which occurs for $V > 7.5t$. This is an unusual behavior for this “superconducting” phase because $S_\rho/S_K = 0$ for a true superconductor.⁴⁹ In the $V \rightarrow \infty$ limit, both Drude weights go to zero because the system becomes phase separated at $V = \infty$ for $U=0$. The lattice is decomposed in finite-size domains of singly occupied or empty sites with an average

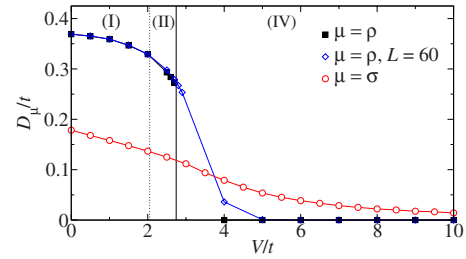


FIG. 5. (Color online) The charge Drude weight D_ρ and spin Drude weight D_σ as a function of V along the $U=10t$ line. Squares and circles are results extrapolated to the thermodynamic limit. Diamonds show finite-system results ($L=60$). The solid vertical line is the phase boundary between the metallic and insulating (IV) states determined by the calculation of K_ρ in Ref. 30. The dashed vertical line marks the boundary between the Luttinger liquid regions with dominant SDW (i) and CDW (II) fluctuations.

electronic density $< 1/2$. These domains are separated by impenetrable immobile walls (the doubly occupied sites). There is a finite density of such pairs for small U because they reduce the average density on the other sites below $1/2$ and thus allow them to gain kinetic energy. The charge Drude weight is zero despite the finite kinetic energy [i.e., $S_K \neq 0$ in Eq. (6)] because charge motion is confined to finite domains by the infinite walls.⁵⁰ Therefore, there are only incoherent contributions to the charge conductivity and $S_\rho = -S_K$. The spin Drude weight must also vanish for this reason and also because the infinite nearest-neighbor interaction V prohibits the formation of any nearest-neighbor electron pairs and thus the effective magnetic interaction is zero.^{24,25}

Exact diagonalization studies²⁴ have shown that the compressibility κ_ρ increases with V in this “superconducting” region and seems to diverge when approaching the phase-separation regime for $V \rightarrow \infty$. As within the TLL approach the compressibility can be characterized by $\kappa_\rho = 2K_\rho / \pi v_\rho$, the divergence of κ_ρ has been interpreted as a divergence of K_ρ . However, our DMRG calculations show that $D_\rho = v_\rho K_\rho / \pi$ decreases as V becomes very large. Thus v_ρ goes to zero faster than K_ρ diverges toward ∞ (if it diverges) and we conclude that the divergence of κ_ρ is mostly due to the vanishing of the charge velocity for $V \rightarrow \infty$. Unfortunately, it is difficult to compute K_ρ using the DMRG method close to the phase-separation regime. Thus we cannot determine whether K_ρ diverges to ∞ or converges to a finite value.

Our results for the $U=10t$ line are shown in Fig. 5. As V increases, there is a phase transition from the metallic state to the $4k_F$ -CDW insulating state at $V_c/t \approx 2.74$.³⁰ In the metallic phase, both Drude weights decrease when V increases and we always find $D_\rho > D_\sigma$ as discussed previously. The spin Drude weight changes smoothly and remains finite for all values of the interaction parameters that we have investigated. As seen in Fig. 5, the charge Drude weight approaches a finite value when $V \rightarrow V_c$ from the metallic side. As $D_\rho = 0$ in the insulating phase for $V > V_c$, we conclude that the charge Drude weight jumps from a finite value to zero at the metal-insulator transition. Therefore, D_ρ is a discontinuous function of the interaction parameters. Note that the finite system $D_\rho(L)$ calculated with DMRG are smooth functions

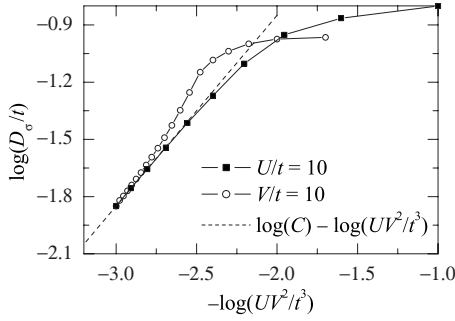


FIG. 6. Spin Drude weight D_σ vs $-\log(UV^2/t^3)$ in the strong-coupling region. Solid lines are guides for the eyes.

of the parameters (see Fig. 5) and from the finite-size scaling analysis alone one cannot determine whether D_ρ has a jump at $V=V_c$ (this will be discussed in detail in the next subsection). The transition from the metallic to the insulating phase is believed to be of the Kosterlitz-Thouless type and to be caused by the $8k_F$ -umklapp scattering.^{19,20} This scattering is different from the usual $4k_F$ -umklapp scattering which reduces the charge velocity v_ρ in renormalization-group calculations and is always irrelevant.^{46,47} Therefore, both v_ρ and K_ρ are renormalized to a finite value when approaching the phase boundary from the metallic side in the renormalization-group analysis.

Unfortunately, our simulations show that it is difficult to determine the phase boundary using the discontinuity in D_ρ . We believe that the direct calculation of K_ρ from correlation functions³⁰ is a more efficient approach for determining phase boundaries within DMRG computations because the extrapolation to infinite system size is less difficult than for the Drude weights. This will be discussed in the following subsection.

In the strong-coupling limit of the insulating CDW phase (IV) electrons are localized and there is an effective Heisenberg-type interaction between their spins. The effective exchange interaction J_{eff} between nearest-neighbor spins can be derived from perturbation theory and we obtain up to fourth order $J_{\text{eff}} \propto t^4/UV^2$. In a Heisenberg model, D_σ is proportional to the exchange interaction. Therefore we expect $D_\sigma = Ct^4/UV^2$ in the strong-coupling limit of our electronic model, where C is an unknown constant. In Fig. 6 we show our numerical results for the strong-coupling limit on a double-logarithmic scale. One can clearly see a linear asymptotic behavior $\log(D_\sigma/t) = \log(C) - \log(UV^2/t^3)$ for large U/t and V/t in agreement with the strong-coupling analysis.

B. Finite-size scaling

With DMRG we have been able to investigate much larger system sizes than in studies based on the exact diagonalization method.^{23–27} Finite-size effects are thus smaller than in these previous studies, and in most cases we can perform a reliable finite-size scaling analysis of DMRG results for finite chains with periodic boundaries and extrapolated to the limit of infinitely long chains. Nevertheless, there are some difficulties close to phase boundaries as usual and it

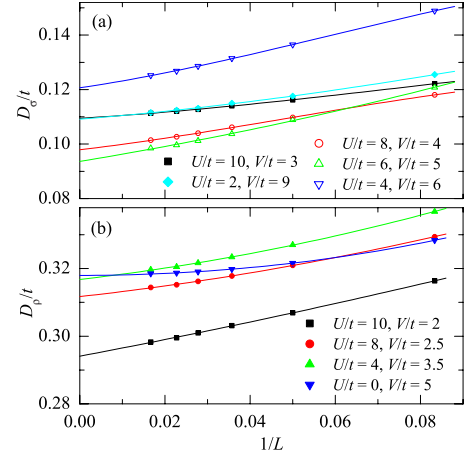


FIG. 7. (Color online) (a) Spin Drude weight D_σ as a function of inverse system length $1/L$ for several parameter sets in the metallic phase (filled symbols) and in the insulating phase (open symbols). Lines are polynomial fits. (b) Charge Drude weight D_ρ for several parameter sets in the metallic phase. Lines are polynomial fits.

is always informative to examine finite-size corrections.

Figure 7(a) shows the spin Drude weight $D_\sigma(L)$ as a function of inverse system length $1/L$ for several parameter sets. We note that $D_\sigma(L)$ decreases monotonically and smoothly with increasing L and also that it converges to a finite value and seems to be a convex function of $1/L$ for $L \rightarrow \infty$ both in the metallic and in the insulating phase. This finite-size scaling reflects the absence of gap in the spin sector and the complete separation of low-energy spin and charge excitations in the quarter-filled extended Hubbard model for $U, V \geq 0$. We can extrapolate the Drude weight to the thermodynamic limit systematically by performing a polynomial fit in $1/L$. We find that the extrapolation is always very well behaved as seen from Fig. 7(a). Especially, the relative errors are small, i.e., the difference between the extrapolated value D_σ and the value of $D_\sigma(L)$ for the largest system size L computed with DMRG is small compared to D_σ .

Figure 7(b) shows the charge Drude weight $D_\rho(L)$ as a function of inverse system length $1/L$ for several parameter sets in the metallic phase. As expected, $D_\rho(L)$ converges to a finite value for $L \rightarrow \infty$. As for the spin Drude weight, we find that finite-size corrections are positive and depend smoothly on L and that $D_\rho(L)$ seems to be a convex function of $1/L$ for $L \rightarrow \infty$. Again such a finite-size scaling reflects the absence of gap in the charge sector in this part of the phase diagram. We can extrapolate $D_\rho(L)$ to the thermodynamic limit systematically using a polynomial fit in $1/L$. This extrapolation is very accurate as demonstrated by the comparison with the exact results obtained from the Bethe ansatz for the Hubbard model (see Fig. 3). We note, however, that leading finite-size corrections are linear in $1/L$ in the $U > V > 0$ region of the parameter space, whereas they are on the order of $1/L^2$ in the Hubbard model.¹⁷ In the $V > U$ region, we find that finite-size corrections to D_ρ are much smaller than for $U > V$ region and that the leading term seems to be again on the order L^{-2} as can be seen for $U=0, V=5t$ in Fig. 7(b).

In Fig. 8(a) we show the charge Drude weight $D_\rho(L)$ in the insulating phase as a function of the system length L for

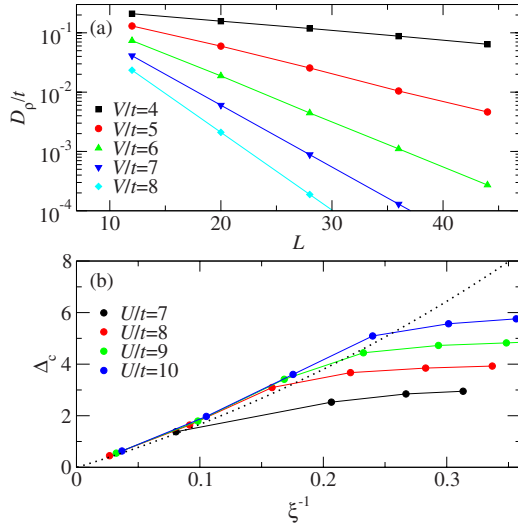


FIG. 8. (Color online) (a) Semilog plot for the charge Drude weight D_ρ at $U/t=10$ as a function of the system size L . Lines are exponential fits. (b) Charge gap Δ_c vs inverse correlation length ξ^{-1} for $U/t=10, 9, 8, 7$ and varying V . Solid lines are guides for the eyes. The dashed line is obtained from the Bethe ansatz solution (Ref. 38) in the limit $U/t=\infty$ as V approaches $2t$ from above.

several parameter sets. The linear behavior observed in this semilog plot indicates that $D_\rho(L)$ decreases exponentially with increasing L as in the Hubbard model at half filling.¹⁷ The correlation length ξ which characterizes this exponential decay $\log[D_\rho(L)/t] = -L/\xi$ depends upon U and V . (We set the lattice constant $a=1$.) Near the metal-insulator phase boundary, one expects that ξ^{-1} should vanish as the charge gap Δ_c . In particular, in the half-filled Hubbard model, it has been shown that $\xi^{-1} = \Delta_c/2t = \Delta_c/v_F$ in the weak-coupling limit $U \ll t$.¹⁷ We have determined the correlation length ξ in our model from the slopes of $\log[D_\rho(L)/t]$ versus L . The charge gap is obtained as the difference of ground-state energies extrapolated to the thermodynamic limit

$$\Delta_c = \lim_{L \rightarrow \infty} \Delta_c(L),$$

$$\Delta_c(L) = [E_L(1,1) + E_L(-1,-1) - 2E_L(0,0)]/2. \quad (18)$$

Here $E_L(N_\uparrow, N_\downarrow)$ denotes the ground-state energy of a chain of length L with N_\uparrow up-spin and N_\downarrow down-spin electrons added or removed from the quarter-filled band, which can be easily computed using the DMRG method. Figure 8(b) shows Δ_c/t vs ξ^{-1} for several values of U and V . We see that ξ^{-1} varies linearly with Δ_c for small gaps, while deviations are apparent when the gap is large. The product $\xi\Delta_c$ tends to a universal value $\xi\Delta_c \approx 13.8t \approx 9.76v_F$ for $\Delta_c \rightarrow 0$ independently of U and V . This agrees with the relation between ξ and Δ_c derived from Bethe ansatz results³⁸ for the effective spinless fermion model which corresponds to our model in the limit $U/t=\infty$ as V approaches $2t$ from above [see the dashed line in Fig. 8(b)].

It is also necessary to discuss the finite-size scaling of the charge Drude weight in the vicinity of the metal-insulator transition in more detail. In Fig. 9 we plot the charge Drude

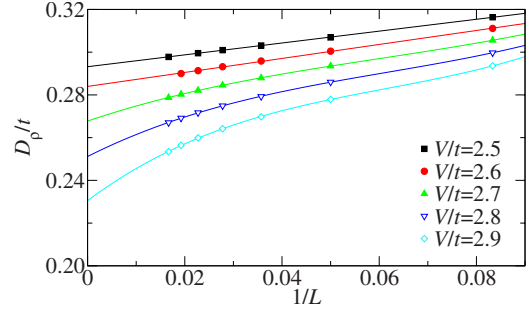


FIG. 9. (Color online) (a) The charge Drude weight D_ρ as a function of inverse system length $1/L$ at $U/t=10$ for various V in the metallic phase (filled symbols, $V < V_c \approx 2.74t$) and in the insulating phase (open symbols, $V > V_c$). Lines are polynomial fit.

weight $D_\rho(L)$ as a function of inverse system length $1/L$ for $U=10t$ and several values of V close to the critical value $V_c \approx 2.74t$ determined in Ref. 30. If we perform a polynomial fit in $1/L$, all results extrapolate to finite values for both phases while an exponential fit is meaningless. Thus from our numerical results alone, we would conclude that D_ρ decreases smoothly as a function of V through the critical value $V_c \approx 2.74t$ determined in Ref. 30 and vanishes only for $V > V^*$, where V^* is clearly larger than V_c .

This failure of our finite-size analysis is easy to understand. Obviously, if we assume a scaling behavior $D_\rho(L) \approx A \exp(-L/\xi)$ in the critical region $V \approx V_c$ of the insulating phase and ξ diverges as $V \rightarrow V_c$, we need to treat exponentially large systems to observe the correct finite-size scaling of $D_\rho(L)$. Therefore, one has to use much larger sizes than the ones used here (up to $L=60$) to determine the phase boundary from the extrapolated charge Drude weights. Unfortunately, it is very difficult to obtain accurate results for larger periodic systems using DMRG. We note that $D_\rho(L)$ seems to be a convex function of $1/L$ in the metallic phase but a concave function in the insulating phase. Although this finite-size behavior could be used as a criterion to distinguish both phases in principle, it is not reliable generally as it does not hold when V is kept fixed and U varies through the critical value U_c . Moreover, this is a transient behavior for intermediate values of $1/L$ only as $D_\rho(L) \approx A \exp(-L/\xi)$ is also a convex function of $1/L$ for large enough $L \gg \xi$ in the insulating phase.

The Luttinger parameter K_ρ also extrapolates to a finite value in the insulating phase if the available system sizes are too small.³⁰ Nevertheless, the direct calculation of K_ρ from the finite-size scaling of correlation functions allows one to determine the metal-insulator phase boundary very accurately because this approach can be applied for open boundary conditions and thus with DMRG, one can simulate systems which are 1 to 2 orders of magnitude larger than with periodic boundary conditions.

V. SUMMARY

We have studied the transport properties of the t - U - V extended Hubbard model at quarter filling by using the DMRG technique combined with a variational principle for the

Drude weight. The contour map of the charge and spin Drude weights has been determined in the parameter space of the on-site Coulomb repulsion U and nearest-neighbor Coulomb repulsion V . We have found that (i) both Drude weights decrease monotonically with increasing Coulomb repulsion, (ii) the charge Drude weight is larger than the spin Drude weight in the metallic phase (Luttinger liquid), and (iii) the charge Drude weight is discontinuous across the Kosterlitz-Thouless transition from the metallic phase to the CDW insulating phase.

We have also discussed the finite-size scaling and the extrapolation to the thermodynamic limit of our numerical data. In the insulating phase, we find a universal relation between the charge gap and the correlation length which controls the exponential decay of finite-size corrections to the charge Drude weight. Unfortunately, we reach the conclusion that it

is difficult to determine the phase boundary of a metal-insulator transition using the Drude weights calculated with DMRG because this approach requires periodic boundary conditions which considerably reduce the performance of DMRG and thus the available system sizes for the finite-size scaling analysis.

ACKNOWLEDGMENTS

We thank S. Ejima and S. Nishimoto for useful discussions. This work was supported in part by Grants-in-Aid for Scientific Research from the Ministry of Education, Science, Sports and Culture of Japan (Grant No. 19.963). A part of the computations was carried out at the Research Center for Computational Science, Okazaki Research Facilities, and the Institute for Solid State Physics, University of Tokyo.

-
- ¹X. Zotos, J. Phys. Soc. Jpn. Suppl. **74**, 173 (2005).
²R. Kubo, J. Phys. Soc. Jpn. **12**, 570 (1957).
³W. Kohn, Phys. Rev. **133**, A171 (1964).
⁴D. Jérôme, Science **252**, 1509 (1991).
⁵H. Seo, C. Hotta, and H. Fukuyama, Chem. Rev. (Washington, D.C.) **104**, 5005 (2004).
⁶T. Lorenz, M. Hofmann, M. Grüninger, A. Freimuth, G. S. Uhrig, M. Dumm, and M. Dressel, Nature (London) **418**, 614 (2002).
⁷H. J. Schulz, in *Strongly Correlated Electronic Materials*, edited by K. S. Bedell, Z. Wang, D. E. Meltzer, A. V. Balatsky, and E. Abraham (Addison-Wesley, Reading, MA, 1994), p. 187.
⁸J. Sólyom, Adv. Phys. **28**, 201 (1979).
⁹V. J. Emery, in *Highly Conducting One-Dimensional Solids*, edited by J. T. Devreese, R. Evrand, and V. van Doren (Plenum, New York, 1979), p. 327.
¹⁰J. Voit, Rep. Prog. Phys. **58**, 977 (1995).
¹¹T. Giamarchi, *Quantum Physics in One Dimension* (Oxford Science, New York, 2004), p. 391.
¹²A. V. Sologubenko, K. Gianno, H. R. Ott, U. Ammerahl, and A. Revcolevschi, Phys. Rev. Lett. **84**, 2714 (2000).
¹³C. Hess, C. Baumann, U. Ammerahl, B. Büchner, F. Heidrich-Meisner, W. Brenig, and A. Revcolevschi, Phys. Rev. B **64**, 184305 (2001).
¹⁴K. Kudo, S. Ishikawa, T. Noji, T. Adachi, Y. Koike, K. Maki, S. Tsuji, and K. Kumagai, J. Phys. Soc. Jpn. **70**, 437 (2001).
¹⁵F. Heidrich-Meisner, A. Honecker, and W. Brenig, Eur. Phys. J. Spec. Top. **151**, 135 (2007).
¹⁶D. Poilblanc, T. Ziman, J. Bellissard, F. Mira, and G. Montambaux, Europhys. Lett. **22**, 537 (1993).
¹⁷C. A. Stafford, A. J. Millis, and B. S. Shastry, Phys. Rev. B **43**, 13660 (1991); C. A. Stafford and A. J. Millis, *ibid.* **48**, 1409 (1993).
¹⁸A. Luther and I. Peschel, Phys. Rev. B **9**, 2911 (1974); D. C. Mattis, J. Math. Phys. **15**, 609 (1974); J. W. Cannon and E. Fradkin, Phys. Rev. B **41**, 9435 (1990); J. Voit, *ibid.* **45**, 4027 (1992).
¹⁹H. Yoshioka, M. Tsuchiizu, and Y. Suzumura, J. Phys. Soc. Jpn. **69**, 651 (2000).
²⁰H. Yoshioka, M. Tsuchiizu, and Y. Suzumura, J. Phys. Soc. Jpn. **70**, 762 (2001).
²¹B. Fourcade and G. Spronken, Phys. Rev. B **29**, 5089 (1984).
²²S. Andergassen, T. Enss, V. Meden, W. Metzner, U. Schollwöck, and K. Schönhammer, Phys. Rev. B **73**, 045125 (2006).
²³L. M. del Bosch and L. M. Falicov, Phys. Rev. B **37**, 6073 (1988); B. Fourcade and G. Spronken, *ibid.* **29**, 5096 (1984).
²⁴F. Mila and X. Zotos, Europhys. Lett. **24**, 133 (1993).
²⁵K. Penc and F. Mila, Phys. Rev. B **49**, 9670 (1994).
²⁶M. Nakamura, Phys. Rev. B **61**, 16377 (2000).
²⁷K. Sano and Y. Ôno, Phys. Rev. B **70**, 155102 (2004).
²⁸J. E. Hirsch, Phys. Rev. Lett. **53**, 2327 (1984); J. E. Hirsch and D. J. Scalapino, Phys. Rev. B **27**, 7169 (1983); **29**, 5554 (1984); H. Q. Lin and J. E. Hirsch, *ibid.* **33**, 8155 (1986); J. W. Cannon, R. T. Scalettar, and E. Fradkin, *ibid.* **44**, 5995 (1991).
²⁹P. Schmitteckert and R. Werner, Phys. Rev. B **69**, 195115 (2004).
³⁰S. Ejima, F. Gebhard, and S. Nishimoto, Europhys. Lett. **70**, 492 (2005).
³¹E. H. Lieb and F. Y. Wu, Phys. Rev. Lett. **20**, 1445 (1968).
³²F. D. M. Haldane, Phys. Rev. Lett. **45**, 1358 (1980); **47**, 1840 (1981); J. Phys. C **14**, 2585 (1981).
³³C. N. Yang and C. P. Yang, Phys. Rev. **150**, 327 (1966).
³⁴M. Fowler and M. W. Puga, Phys. Rev. B **18**, 421 (1978).
³⁵Y. Suzumura, J. Phys. Soc. Jpn. **66**, 3244 (1997).
³⁶P. Chandra, P. Coleman, and A. I. Larkin, J. Phys.: Condens. Matter **2**, 7933 (1990).
³⁷P. Kopietz, Phys. Rev. B **57**, 7829 (1998).
³⁸B. S. Shastry and B. Sutherland, Phys. Rev. Lett. **65**, 243 (1990).
³⁹A. J. Millis and S. N. Coppersmith, Phys. Rev. B **42**, 10807 (1990).
⁴⁰R. M. Fye, M. J. Martins, D. J. Scalapino, J. Wagner, and W. Hanke, Phys. Rev. B **44**, 6909 (1991).
⁴¹P. Kopietz, Mod. Phys. Lett. B **7**, 1747 (1993).
⁴²E. Jeckelmann, Phys. Rev. B **66**, 045114 (2002).
⁴³E. Jeckelmann and H. Benthien, in *Computational Many Particle Physics*, Lecture Notes in Physics Vol. 739, edited by H. Fehske, R. Schneider, and A. Weiße (Springer-Verlag, Berlin, Heidelberg, 2008), pp. 621–635.

- ⁴⁴E. Jeckelmann, Phys. Rev. B **67**, 075106 (2003).
- ⁴⁵F. C. Dias, I. R. Pimentel, and M. Henkel, Phys. Rev. B **73**, 075109 (2006).
- ⁴⁶T. Giamarchi, Phys. Rev. B **44**, 2905 (1991).
- ⁴⁷T. Giamarchi, Phys. Rev. B **46**, 342 (1992).
- ⁴⁸A. V. Chubukov, D. L. Maslov, and F. H. L. Essler, Phys. Rev. B **77**, 161102(R) (2008).
- ⁴⁹D. J. Scalapino, S. R. White, and S. Zhang, Phys. Rev. B **47**, 7995 (1993).
- ⁵⁰M. Rigol and B. S. Shastry, Phys. Rev. B **77**, 161101(R) (2008).